IEEE Access
Multidisciplinary | Rapid Review | Open Access Journal

Received November 24, 2021, accepted December 20, 2021, date of publication December 30, 2021,
date of current version January 7, 2022.

Digital Object Identifier 10.1109/ACCESS.2021.3139828

Ultra-Wideband Hybrid Magneto-Electric Dielectric-Resonator Dipole Antenna Fed by a Printed RGW for Millimeter-Wave Applications

MOHAMED MAMDOUH M. ALI[1,2], (Member, IEEE),
MUATH AL-HASAN[3], (Senior Member, IEEE),
ISMAIL BEN MABROUK[4], (Senior Member, IEEE),
AND TAYEB A. DENIDNI[1], (Fellow, IEEE)

[1]Institut National de la Recherche Scientifique (INRS), Universite du Quebec, Montreal, QC H5A 1K6, Canada
[2]Electrical Engineering Department, Assiut University, Assiut 71515, Egypt
[3]Department of Electrical Engineering, Al Ain University of Science and Technology, Abu Dhabi, United Arab Emirates
[4]Department of Electrical Engineering, Durham University, Durham DH1 3DE, U.K.

Corresponding author: Mohamed Mamdouh M. Ali (mohamed.ali@ieee.org)

ABSTRACT Future communication standards have an increasing interest in Millimeter Wave (mm-wave) bands, where wide bandwidth and secured communication can be assured. This trend in communication standards stimulates the research community to provide novel antenna configurations in the mm-wave bands. This article proposes a novel design and analysis of hybrid magneto-electric dielectric-resonator dipole antenna that features an electrically small size with ultra-wideband operation and consistent radiation characteristics in the mm-wave band. The proposed antenna is designed based on the combination of multi-resonances produced by a Magneto-Electric (ME) dipole and stacked Dielectric Resonator Antennas (DRAs). In addition, the proposed antenna is implemented using state-of-the-art Printed Circuit Board (PCB) technology, namely, Printed Ridge Gap Waveguide (PRGW) for low loss and cost-efficiency. The combination between the ME-dipole and stacked DRA is adopted to ensure symmetric radiation characteristics in both E- and H-planes over ultra-wideband operation with a deep matching level. Both DRA and ME-dipole elements are designed and studied separately, where a systematic design procedure is presented to obtain initial design parameters. Proper integration between the radiating elements introduced an electrically small size antenna ($0.64\,\lambda \times 0.48\lambda$) covers the full Ka-band (26-40 GHz) with a matching level beyond -20 dB and gain stability of 8 ± 1 dB. The antenna prototype is fabricated, where a good agreement is shown between both simulated and measured results.

INDEX TERMS Dielectric resonator antenna (DRA), magneto-electric (ME) dipole, printed ridge gap waveguide (PRGW).

I. INTRODUCTION

Future communication systems have received significant attention, where more subscribers with higher data-rate for each user need to be covered. This attracts system engineers to deploy higher frequency bands that support short-range communication with ultra-wideband operation. This direction in future communication must be supported by the development of various microwave components and antenna systems in mm-wave bands [1], [2]. Accordingly, massive efforts have been directed by the microwave/ antenna researchers for designing mm-wave structures over the past decade, proposing various configurations for passive microwave components [3]–[5], active circuits [6] and antenna elements [7], [8].

Low-profile printed antennas are essential building blocks for modern communication systems in mm-wave bands, where both cost and size are critical features. The printed antennas have been addressed extensively based on either classical guiding structure such as microstrip lines [9]–[12] or modern technology such as substrate integrated waveguide (SIW) [13]–[16]. Although the classical guiding structure-based antennas can provide the required bandwidth and compactness with a cost-effective solution in low-frequency

The associate editor coordinating the review of this manuscript and approving it for publication was Davide Ramaccia.

bands; however, the dielectric and radiation losses are significant and have more impact at higher frequency bands, which limits their applications at mm-wave bands. On the other hand, the radiation losses can be significantly reduced through the utilization of SIW technology, where the signal is fully confined between two metallic plates and guided from both sides by periodic vias. However, dielectric losses represent a huge drawback in this technology as the signal propagates inside the dielectric region. Another promising structure is the printed ridge gap waveguide (PRGW), where the radiation and dielectric losses are reduced through the propagation in an air gap above the ridge surrounded by periodic electromagnetic band-gap cells [17]–[19]. This state-of-the-art guiding structure has attracted great interest from the research community especially in mm-wave bands introducing various microwave components and antenna configurations. However, there is still a significant room of improvement in the performance of these components to overcome the associated challenges reported in the literature.

Recently, various mm-wave PRGW based antenna designs have been reported in the literature, which is separately deploying either ME-dipole or DRA configurations. Each of these antenna types has its advantages which include a wide bandwidth and symmetrical E- and H-plane stable radiation characteristics for ME-dipole [8], [23] or electrically small size and high efficiency for DRA configurations [11], [12]. For example, some presented antenna structures have sacrificed the bandwidth to provide a high gain solution [8], [20]–[22]. Others proposed antenna configurations that cover a wide bandwidth, nonetheless, with unstable gain [23], [24]. Moreover, most of the published configurations that have deployed dielectric resonator structures do not maintain symmetrical radiation characteristics over a wide operating bandwidth [25]–[27]. Therefore, introducing a novel type of mm-wave antenna incorporating both ME-dipole and DRA features is essential to elevate the performance of future wireless communication systems.

In this article, we propose the design and analysis of a novel Hybrid Magneto-Electric Dielectric-Resonator Dipole (ME-DRD) antenna based on PRGW technology for mm-wave applications. The proposed antenna achieves an outstanding performance due to the combination of the two fundamental types of radiators, namely, ME-dipole and DRA. As a result, the proposed antenna is achieved not only an ultra-wide bandwidth, identical E/H-plane, stable gain, compact size but also a deep matching level (<-20 dB) compared with other published designs. The main radiators for the proposed antenna are well studied and designed separately, where the dimensions of the geometrical configuration parameters are calculated based on the required resonance frequency through the operating bandwidth. Proper integration between the proposed antenna elements was performed, where the proposed ME-DRD antenna is tuned to achieve a deep matching level below -20 dB covering the frequency range of 26-40 GHz. In addition, the proposed antenna configuration produces symmetric radiation characteristics

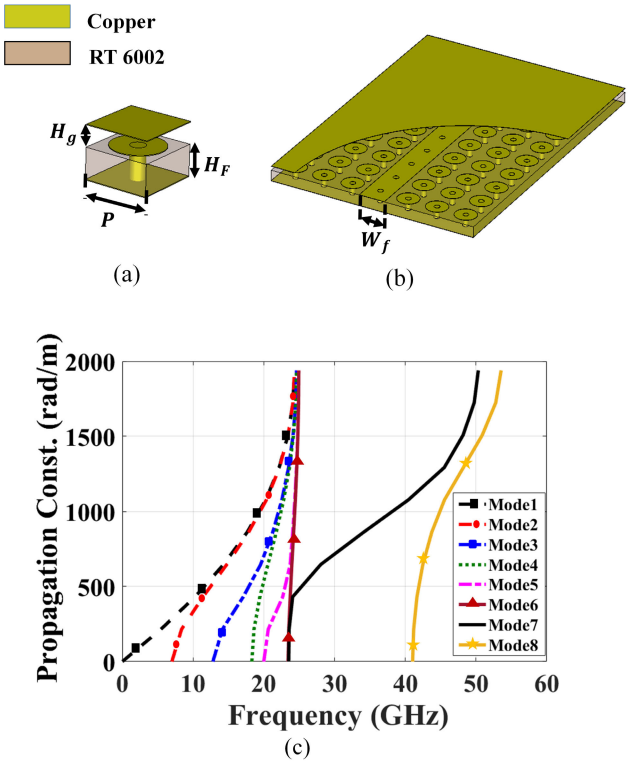

FIGURE 1. The proposed PRGW structure. (a) The proposed EBG unit cell. (b)The proposed PRGW line. (c) The dispersion diagram.

over the suggested bandwidth. Furthermore, a stable gain of 8 ± 1 dB is achieved over the operating bandwidth with a compact size of ($0.64\ \lambda \times 0.48\lambda$). To the best of the authors' knowledge, the proposed antenna configuration outperforms the published antenna structures in the literature, where a detailed comparison between this work and other related published contributions is addressed in detail.

This article is organized as follows: In Section III, the proposed structure is presented along with the analysis of the antenna modes. This is followed by a detailed discussion on the fabricated prototype, where the comparison between the measured and the simulated response is criticised in Section IV. In Section V, the performance of the antenna is evaluated through a comparison with other related published work to highlight the proposed antenna edge. Finally, the outcomes of this work is summarized in Section VI.

II. PROPOSED PRGW STRUCTURE DESIGN AND EXCITATION

The proposed antenna consists of PRGW antenna connected to a PRGW feeding line, where in a later section this feeding line will be connected to a standard connector for measurement purposes. The PRGW feeding line is designed with a cell size of $P = 1.7$ mm and a patch radius of $r = 0.7$ mm. The designed cell is printed on Roger RT 6002 substrate with a height of $H_F = 0.762$ mm, while the via diameter is 0.38 mm. The proposed unit cell, as well as the straight PRGW feeding line, are shown in Fig. 1(a) and 1(b),

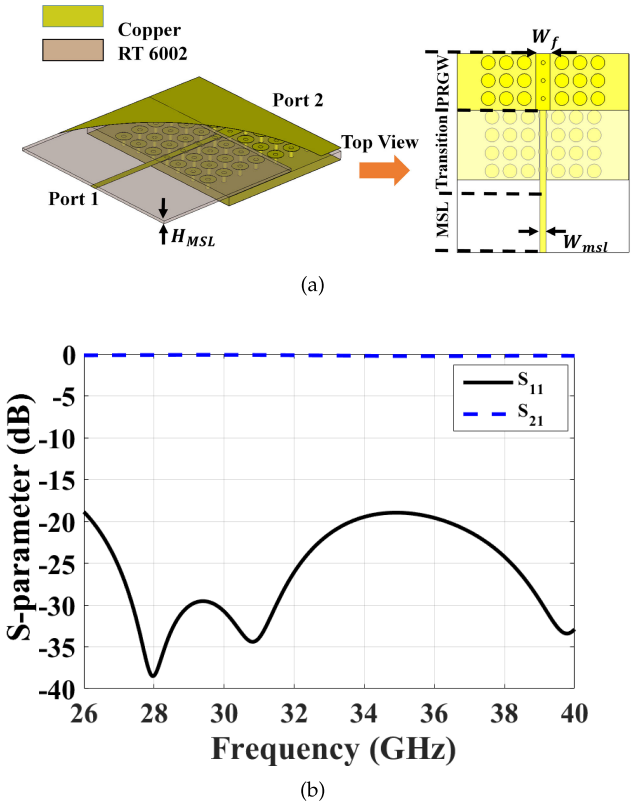

FIGURE 2. (a) The proposed microstrip line to PRGW transition. (b) The simulated S-parameter of the proposed transition.

respectively. These parameters are deployed to model the PRGW, where the simulated modes with the presence of the ridge are shown in Fig. 1(c). It can be depicted form this figure that a quasi-TEM mode exists in the frequency band from 23 GHz to 40 GHz, which is a bit larger than the suggested frequency band. Accordingly, this PRGW cell configuration provides a suitable guiding structure for the antenna design. The second part of the proposed transition is a Microstrip line to PRGW transition, where the middle strip is connected to the printed ridge through a matching section as shown in Fig. 2(a). The utilized matching section is simple and effective, where the microstrip line is connected to a dielectric filled PRGW, which in turns, is connected to the air filled PRGW. The width of the intermediate section is used as a tuning parameter to achieve the required matching level. The simulated response of the entire transition is shown in Fig. 2(b), where a matching level better than -19 dB is achieved over the entire frequency band. In the next section, the proposed antenna design, fed by this PRGW, is discussed.

III. PROPOSED ANTENNA DESIGN

The proposed ME-DRDA antenna structure, shown in Fig. 3 consists of two basic elements: a ME-dipole and two-layered DRA loading. Both elements are selected to produce symmetrical radiation patterns, which is a mandatory condition to have a stable radiation characteristics over an ultra-wide bandwidth. It is worth mentioning that, it is

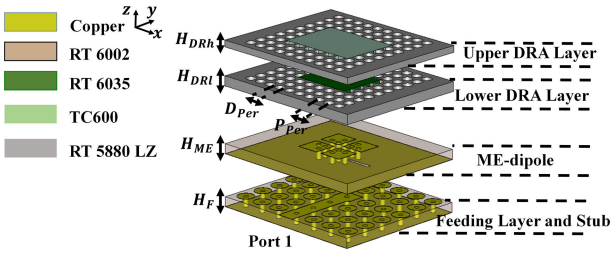

FIGURE 3. The geometrical configuration of the proposed antenna fed by PRGW Line.

hard to achieve a sufficient matching level if the proposed configuration is only fed by a slot deployed in the ME-dipole ground plane. Therefore, the integration between these radiators is fed through a PRGW line terminated with a wide bandwidth hexagonal-shaped open stub located in the bottom layer, as shown in Fig. 3. This section is divided into three subsections:the first two subsections discuss the two antenna basic elements, while the third subsection presents the integration and the realization methodology.

A. PRGW ME-DIPOLE ANTENNA DESIGN

The ME-dipole antenna is selected to be one of the main radiators of the proposed ME-DRD Antenna as it offers a superior radiation characteristics compared to other radiators, such as slot or electric dipoles antennas. The ME-dipole is an integration between a printed dipole and a slot simultaneously excited, where each component is responsible of a certain specific resonance. These two resonances can be adjusted to overlap each other and provide a wide bandwidth; however, it is not sufficient to cover, for example, the whole Ka-band with a reasonable matching level.

Although the printed ME-dipole antenna design is presented several times in the literature, the design procedures have not been described in details. To get an initial estimate for the proposed ME dipole dimensions shown in Fig. 4(a), we assume a dipole arm length of quarter wavelength and a slot length of half wavelength. As a result, the dimensions of both the dipole arm and the slot can be written as follow:

$$L_{Ed} = \frac{C}{4f_{oh}\sqrt{\varepsilon_{r1eff}}} - \frac{H_{ME}}{\sqrt{\varepsilon_{r1}}} \quad (1)$$

$$L_{Md} = \frac{C}{2f_{ol}\sqrt{\varepsilon_{r1eff}}} \quad (2)$$

where, C is the velocity of light, f_{ol} and f_{oh} are the lower and higher resonance frequencies, respectively, ε_{r1} is the dielectric constant of Roger RT6002, and $\varepsilon_{r1eff} = \frac{\varepsilon_{r1}+1}{2}$ is the ME-dipole effective dielectric constant. Afterwards, the dimensions are selected to allocate the two resonances at 28 GHz and 40 GHz, respectively, where the proposed ME-dipole return loss is shown in Fig. 4(b). For further clarification on the operation of the proposed ME-dipole, both electric and current distributions are plotted in the same figure. It can be noticed that current distribution is concatenated on the ME-dipole patches which represents the electric dipole, while the electric field is distributed along the

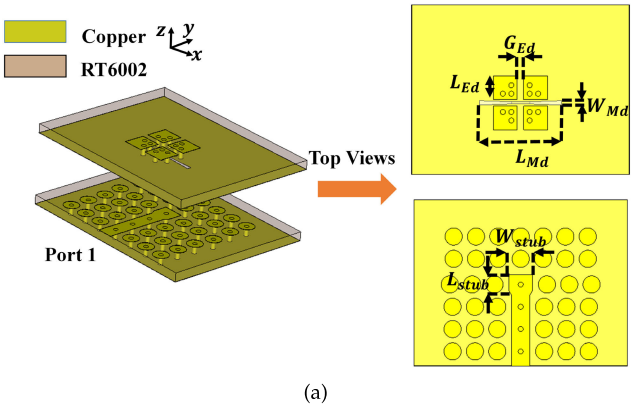

(a)

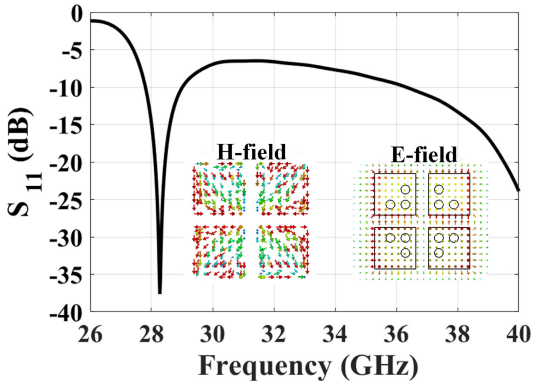

(b)

FIGURE 4. (a) The proposed ME-dipole antenna fed by PRGW Line. (b) The simulated S-parameter of the proposed ME-dipole antenna.

gap between the patches, which confirms the magnetic dipole operation.

B. PRGW DRA ANTENNA DESIGN

The other radiator adopted to improve the performance of the proposed ME-DRD antenna is the DRA as it has smaller size and provides more degrees of freedom as many as available low-cost material products. In addition, it is suitable for mm-wave frequency bands as it is featured with a high efficiency due to the absence of metallic surfaces. The loaded antenna with the DRA is illustrated in Fig. 5(a), which basically consists of two cascaded dielectric resonators on the top of the slot antenna. This DRA configuration is an aperture coupled through the same ME-dipole slot to excite the fundamental mode TE_{111}. The DRA loading is responsible of the third and fourth resonances to further widen the operating bandwidth. These resonances are chosen to occur in between the ME-dipole resonances to ensure a sufficient matching level over the operating bandwidth. The resonant frequency of the fundamental mode $f_{odr1,TE_{111}}$ can be calculated for the lower DRA as follows:

$$f_{odr1} = \frac{C}{2\pi\sqrt{\varepsilon_{r1eff}}}\sqrt{K_x^2 + K_y^2 + K_z^2} \tag{3}$$

$$k_y = \frac{\pi}{L_{DRl}} \tag{4}$$

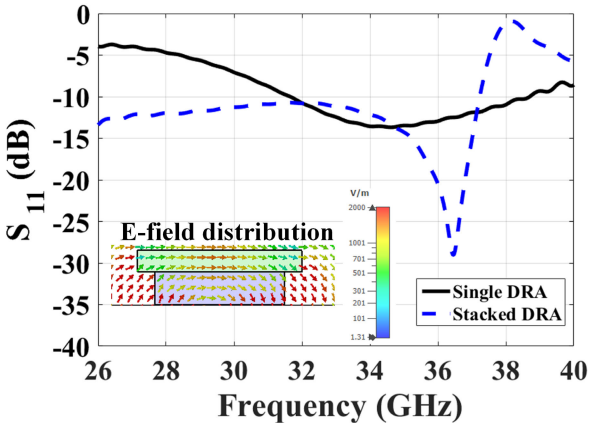

(a)

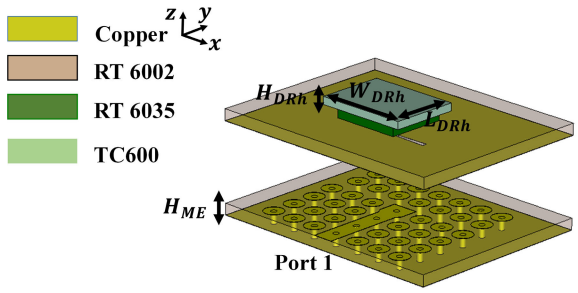

(b)

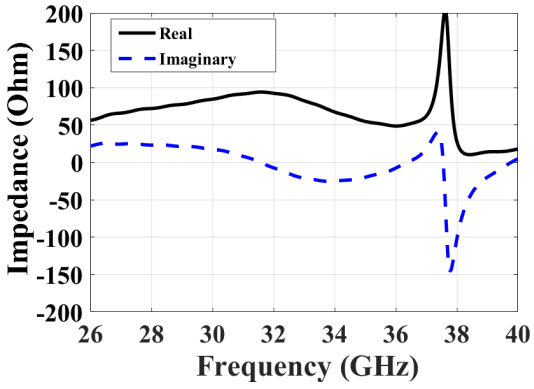

(c)

FIGURE 5. (a) The proposed stacked DRA antenna fed by PRGW Line. (b) The simulated S-parameter of the proposed stacked DRA antenna. (c) The simulated input impedance of the proposed stacked DRA antenna.

$$k_z = \frac{\pi}{2(H_{DRl} + H_{ME})} \tag{5}$$

$$k_x = \frac{2}{W_{DRl}}\tan^{-1}\left(\frac{\sqrt{(\varepsilon_{r2eff} - 1)k_o^2 - k_x^2}}{k_x}\right) \tag{6}$$

where, C is the speed of light and k_o is the free space wave number. An effective dielectric constant for the proposed DRA antenna is calculated as the DRA is placed on the ME-dipole substrate which has different dielectric constant. Therefore, the effective dielectric constant ε_{r2eff} is calculated

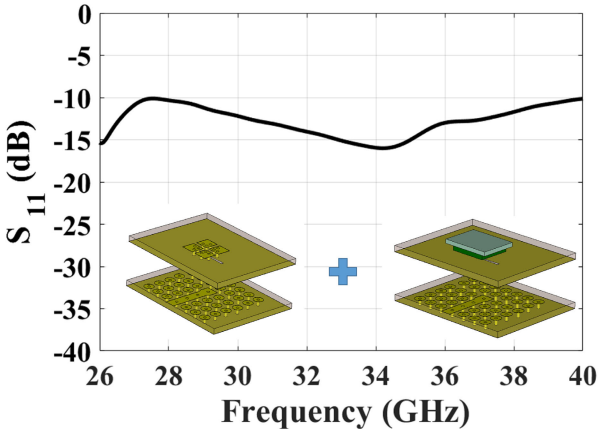

FIGURE 6. The initial simulated S-parameters of the proposed antenna.

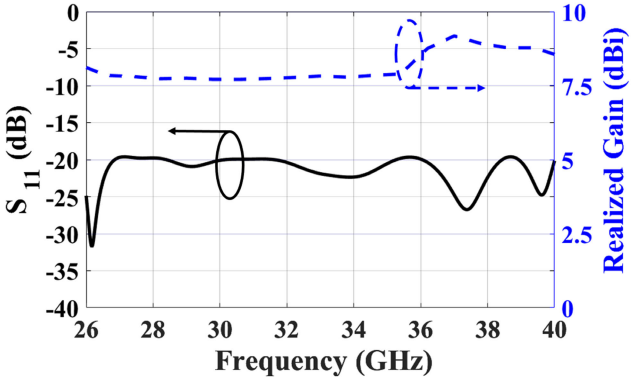

FIGURE 7. The optimized simulated S-parameters and gain of the proposed antenna.

as follow:

$$\varepsilon_{r2eff} = \left(\frac{H_{DRl}}{H_t}\right)\varepsilon_{r2} + \left(1 - \frac{H_{DRl}}{H_t}\right)\varepsilon_{r1} \tag{7}$$

where, $H_t = H_{DRl} + H_{ME}$, ε_{r1} and ε_{r2} are the dielectric constant of Rogers RT6002 and RT6035, respectively. Equations (3-7) are used to estimate initial values of the dimensions of the dielectric resonators in order to resonate around 26 GHz and 34 GHz for the upper and lower DRAs, respectively. The response of the proposed DRA is shown in Fig. 5(b), which highlights a potential resonance at 34 GHz for a single DRA, and dual resonances at 26 GHz and 34 GHz for a stacked DRA as shown in Fig. 5(c). However, as can be observed in Fig. 5(b), by adding the upper DRA, the resonance frequency of the lower DRA is slightly shifted to 36 GHz. In addition, the side view of the simulated E-field distribution of the propose DRA is depicted in Fig. 5(b), where the field distribution is similar to the ideal TE_{111} mode of the rectangular DRA.

C. INTEGRATION AND FABRICATION CONSIDERATIONS

The integration between both main radiators is carried out through staking both structures with the initial dimensions. Based on several parametric studies, we found that the configuration of larger DRA on the top of smaller one results in a good matching level for the proposed antenna

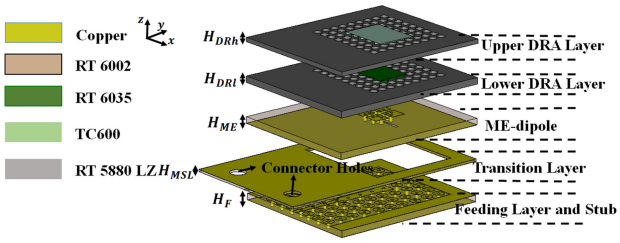

(a)

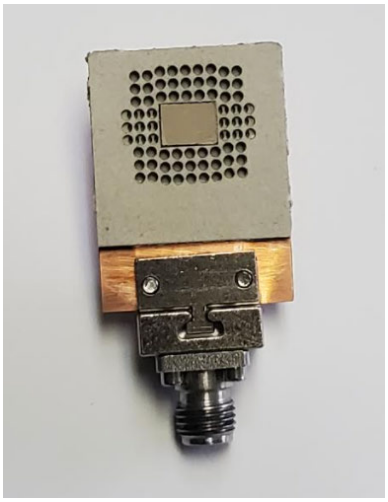

(b)

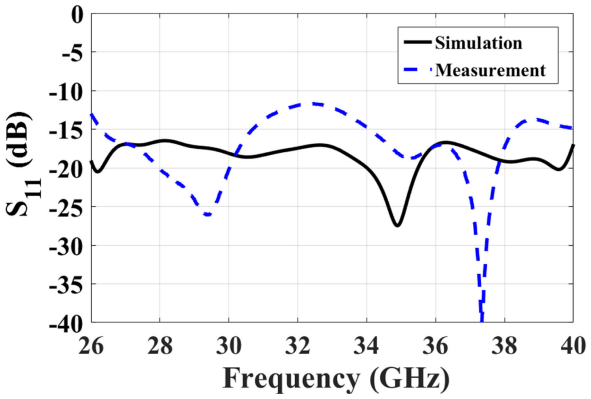

(c)

FIGURE 8. (a) The 3-D model of the proposed antenna. (b) The fabricated prototype of the proposed antenna. (c) Simulated and measured S-parameter of the proposed antenna.

rather than the opposite direction. Gradually increasing the aperture size will allow a smooth transition or radiation of the electromagnetic wave to the free space. In addition, this will increase the gain of the antenna as we will have a larger aperture. The initial response is promising where a matching level below −10 dB is achieved over the operating bandwidth as illustrated in Fig. 6. Hence, an optimization process is performed to obtain a sufficient matching level with a stable gain. The response after optimization for both the gain and the return loss is shown in Fig. 7, where a matching level below −20 dB with a gain stability of ±1 dB is achieved

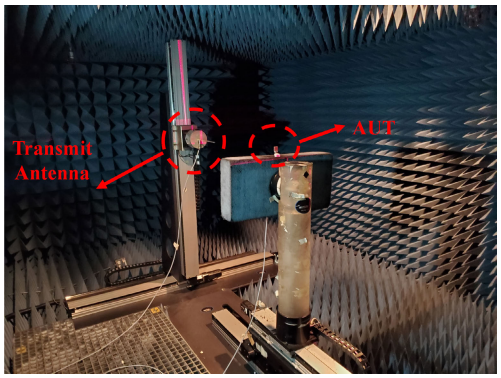

(a)

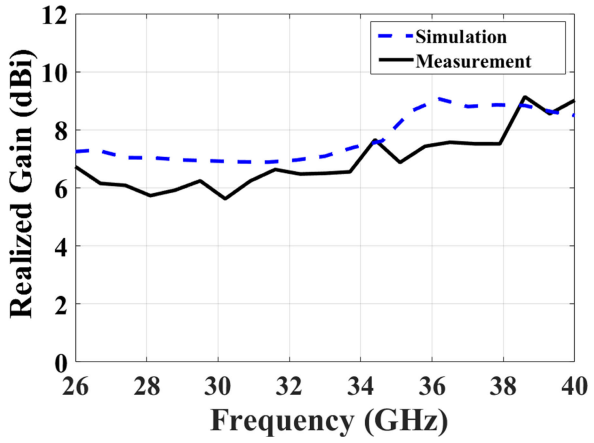

(b)

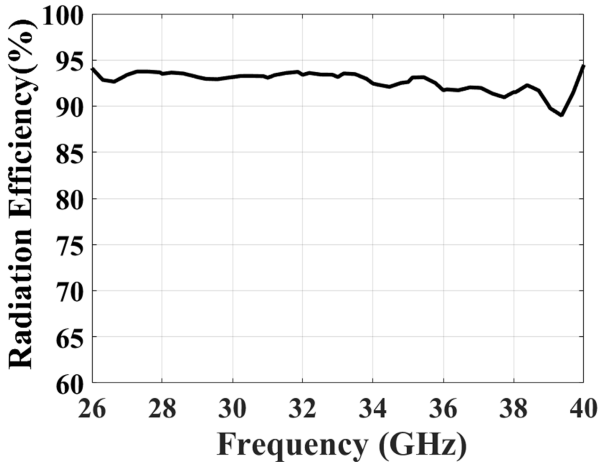

(c)

FIGURE 9. (a) The radiation characteristics measurement setup. (b) Simulated and measured gain of the proposed antenna. (c) Simulated radiation efficiency of the proposed antenna.

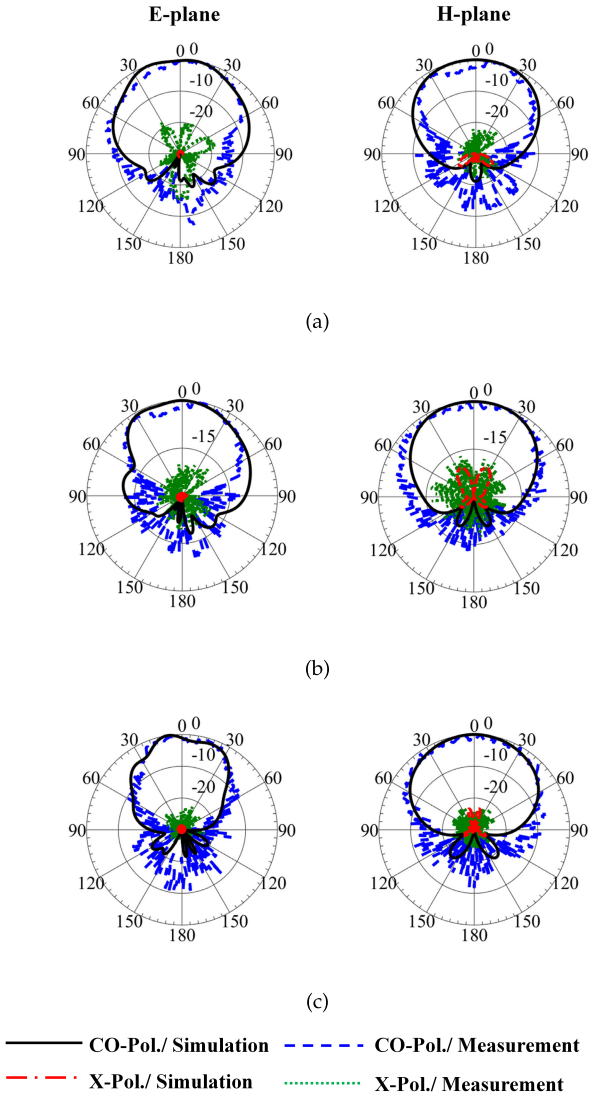

(a)

(b)

(c)

FIGURE 10. Simulated and measured 2-D radiation pattern at different frequencies of the proposed antenna. (a) f=26 GHz. (b) f=33 GHz. (c) f=40 GHz.

TABLE 1. The dimensions of the proposed antenna.

Parameter	H_g	H_f	H_{MSL}	H_{ME}	H_{DRl}
Value	0.289	0.762	0.254	0.762	0.762
Parameter	W_f	W_{MSL}	W_{stub}	W_{MD}	W_{DRl}
Value	1.37	0.6	1.75	0.32	4.67
Parameter	L_{stub}	L_{ED}	L_{MD}	L_{DRl}	L_{DRh}
Value	1.32	1.86	5.9	4.1	4.35

over the whole Ka band. It is worth to mention that the adopted technique to design the proposed antenna results in a deep matching level (<−20 dB) over the whole Ka-band, which is higher than any ME-dipole or DRA that reported in the literature, where −10 dB is the achieved matching level. Thanks for the combination between the ME-dipole and DRA, which results in a novel antenna with superior characteristics. The realization of the proposed antenna is performed through inserting the high dielectric constant material forming the DRA inside a perforated substrate as shown in Fig. 3. This is deployed to ensure the alignment through the fabrication process. The relative permittivity of

TABLE 2. Comparison Between Millimeter Ridge Gap Waveguide Antenna Configuration.

Implementation technology	Frequency (GHz)	Antenna type	Impedance bandwidth	Peak Gain	Size $\lambda \times \lambda$
Printed Ridge Gap Waveguide Waveguide [19]	30	ME-dipole	20%	6 dBi $\pm$ 1	0.5 $\times$ 0.5 $\times$ 0.17
Packaged Microstrip Line [23]	30	ME-dipole	20%	5 dBi$\pm$ 2	1.1 $\times$ 1 $\times$ 0.283
Substrate Integrated Gap Waveguide [21]	26	ME-dipole	29%	8 dBi$\pm$ 2.7	0.8 $\times$ 0.8 $\times$ 0.13
Printed Ridge Gap Waveguide Waveguide [8]	30	ME-dipole with PMC cavity	23.4%	10 dBi $\pm$ 1	1.2 $\times$ 1.2 $\times$0.279
Inverted Microstrip Printed Gap Waveguide [20]	31.5	ME-dipole loaded by SRRs	28%	5.5 dBi$\pm$ 2.5	N.A
Inverted Microstrip Printed Gap Waveguide [22]	31	ME-dipole loaded by SRRs	25%	6 dBi$\pm$ 1	N.A
Inverted Microstrip Printed Gap Waveguide [24]	33	ME-dipole loaded by SRRs	40%	7.5 dBi$\pm$ 3.5	N.A
Printed Ridge Gap Waveguide Waveguide [25]	60	DRA	20%	7.25 dBi$\pm$ 2.25	2.4 $\times$ 2.4 $\times$ 0.254
Printed Ridge Gap Waveguide Waveguide [26]	28	DRA	3.5%	5.36 dBi	N.A
Printed Ridge Gap Waveguide Waveguide [27]	60	DRA	1.6%	7.82 dBi	0.8 $\times$ 0.8 $\times$ 0.414
Printed Ridge Gap Waveguide Waveguide (This Work)	30	ME-dipole loaded DRA	42%	8 dBi $\pm$ 1	0.64 $\times$ 0.48 $\times$ 0.31

the holding substrate is calculated as follow:

$$\varepsilon_{reff-holder} = (1-\alpha)\varepsilon_{r4} + \alpha \tag{8}$$

$$\alpha = \frac{\pi}{2\sqrt{3}}\left(\frac{D_{Per}}{P_{Per}}\right)^2 \tag{9}$$

where, ε_{r4} is the dielectric constant of Rogers RT 5880 LZ. Table 1 indicates the final optimized dimensions of the proposed antenna after the optimization process.

IV. FABRICATION AND EXPERIMENTAL VALIDATION

The proposed ME-DRD antenna structure shown in Fig. 8() is fabricated using the conventional PCB process, and combined together using epoxy at high temperature and pressure [28]. A standard SouthWest Microwave 2.92mm connector is used to test the fabricated prototype as shown in Fig. 8(b). The prototype is measured for the return loss and gain, where a good agreement is achieved between the simulated and the measured response in Fig. 8(c). The proposed antenna achieved a measured matching level of -13 dB over a 42% relative bandwidth at 33 GHz that covers the whole Ka-band. However, a slight discrepancies can be observed for the measured results, which is probably due to fabrication tolerances. More specifically, the epoxy used to assemble the layers, and the soldering that used to ensure the electric contact between the ridge line and the microstrip line. Another factor that may cause the difference between the simulation and the measurement is the changing of the materials dielectric constants at mm-wave frequency compared with the written in the substrate data sheet that are evaluated at 10 GHz. The radiation characteristics of the fabricated antenna are measured inside an anechoic chamber, where the measured setup is shown in Fig. 9. The gain of the fabricated antenna is measured, where a good agreement compared to the simulated results can be observed

in Fig. 9(b). The proposed antenna provides a gain of 8 dBi ± 1 dBi in the whole operating frequency band. Moreover, the radiation patterns were measured and compared with the simulated ones at three different frequencies as shown in Fig. 10. This figure demonstrates that both simulated and measured results are in a good agreement, where the discrepancy between the results is caused by the inaccuracy or misalignment in the radiation pattern measurement setup. The proposed antenna has a symmetrical radiation pattern with a sidelobe level less than −15 dB and a low cross-polarization level less than −20 dB are achieved over the whole frequency band. The radiation pattern is symmetrical in both E- and H planes and stable, which are the main characteristics of such novel hybrid technique that used in this work.

V. PERFORMANCE EVALUATION

Multiple designs have been proposed based on ME-dipoles or dielectric resonators at mm-wave bands in the literature. Several articles have introduced ME-dipole to cover wideband operation around 30 GHz based on printed ridge gap waveguide, packaged microstrip line, and substrate integrated gap waveguide technologies [19], [21], [23]. The bandwidth of such designs is around 20% with a gain in the range of 5 to 8 dB with large variation over the operating bandwidth. Other designs enhanced both the gain and the bandwidth through loading the ME-dipole with Split Ring Resonators (SRR) or PMC surfaces [8], [20], [22], [24]. These techniques can widen the bandwidth up to 40 % and increase the gain by 2 dB. However, the size of the antenna and gain variation increase significantly, which represent obvious drawbacks to these techniques. In addition, most of these designs are using inverted microstrip line that requires an insertion of a substrate layer above the mushroom surface, which adds more space between the mushrooms and the upper ground. Therefore, the dielectric loss is scientifically increased compared with the case of printed RGW used in the proposed work. On the other hands, various antenna designs based on dielectric resonators have been proposed in mm-wave bands, where most of these designs have a narrow bandwidth [25]–[27]. The proposed design in this work gives an excellent compromise, where the bandwidth is featured among all published work in a very compact size. In addition, the presented design provides a stable gain over the operating bandwidth. Furthermore, the proposed ME-DRD antenna is achieved a deep matching level compared with other published designs. This comparison is summarized in Table 2, where the gain, size, bandwidth and the host guiding structure are listed.

VI. CONCLUSION

In this paper, the design and analysis of a novel antenna configuration, namely, ME-DRD antenna fed by printed ridge gap waveguide in mm-wave frequency bands has been proposed. The proposed antenna has been designed through loading a slot with ME-dipole and stacked dielectric resonators to achieve an electrically small size and stable gain with ultra wideband operation. The printed ridge gap waveguide has been adopted to feed the antenna, where low loss and cost efficiency can be achieved. A systematic design procedure has been presented to obtain initial dimensions for the resonators used to construct the proposed antenna. The antenna prototype has been fabricated and tested, where a measured deep matching level and stable gain of 8 dBi ± 1 dBi over the whole operating bandwidth have been achieved. The obtained experimental results have shown a good agreement with those from simulation.With these promising features, the proposed antenna can be a good candidate for future wireless communication systems operating at millimeter-wave bands. The idea of this new type of antenna design could be extended to either mm-wave MIMO antenna systems or high-gain antenna arrays.

REFERENCES

[1] T. Cella, P. Orten, and T. Ekman, "MM-wave short range outdoor links with phased arrays," in *Proc. 6th Int. Symp. Commun., Control Signal Process. (ISCCSP)*, Athens, Greece, May 2014, pp. 214–217.

[2] X. Pu, Y. Tang, S. Shao, and K. L. Law, "On the capacity for 3D LOS MIMO channels in short-range millimeter wave communications," in *Proc. 11th Int. Conf. Wireless Commun., Netw. Mobile Comput. (WiCOM)*, Shanghai, China, 2015, pp. 1–6.

[3] M. M. M. Ali, S. I. Shams, M. Elsaadany, and A. Sebak, "Printed RGW 3-dB backward coupler for millimeter wave applications," in *Proc. IEEE Int. Symp. Antennas Propag. North Amer. Radio Sci. Meeting*, Montreal, QC, Canada, Jul. 2020, pp. 1875–1876.

[4] M. Elsaadany, M. M. M. Ali, S. I. Shams, T. A. Denidni, and G. Gagnon, "A novel design technique for mm-wave mismatch terminations," *IEEE Trans. Microw. Theory Techn.*, vol. 69, no. 3, pp. 1559–1566, Mar. 2021.

[5] M. Y. Soliman, M. M. M. Ali, S. I. Shams, M. F. A. Sree, D. E. Fawzy, and A. M. M. A. Allam, "Ridge gap waveguide wideband hybrid directional coupler for Ka-band applications," in *Proc. 7th Int. Conf. Electr. Electron. Eng. (ICEEE)*, Antalya, Turkey, Apr. 2020, pp. 211–214.

[6] S. I. Shams, M. M. M. Ali, A. Sebak, M. Elsaadany, G. Gagnon, D. E. Fawzy, and A. M. M. A. Allam, "Interfacing wideband amplifiers using ridge gap waveguide for mm-wave systems," in *Proc. 7th Int. Conf. Electr. Electron. Eng. (ICEEE)*, Antalya, Turkey, Apr. 2020, pp. 202–205.

[7] S. M. Sifat, M. M. M. Ali, S. I. Shams, and A.-R. Sebak, "High gain bow-tie slot antenna array loaded with grooves based on printed ridge gap waveguide technology," *IEEE Access*, vol. 7, pp. 36177–36185, 2019.

[8] M. M. M. Ali, I. Afifi, and A.-R. Sebak, "A dual-polarized magneto-electric dipole antenna based on printed ridge gap waveguide technology," *IEEE Trans. Antennas Propag.*, vol. 68, no. 11, pp. 7589–7594, Nov. 2020.

[9] H. Lee, D.-J. Woo, and S. Nam, "Compact and bandwidth-enhanced asymmetric coplanar waveguide (ACPW) antenna using CRLH-TL and modified ground plane," *IEEE Antennas Wireless Propag. Lett.*, vol. 15, pp. 810–813, 2016.

[10] N. Ghassemi, K. Wu, S. Claude, X. Zhang, and J. Bornemann, "Compact coplanar waveguide spiral antenna with circular polarization for wideband applications," *IEEE Antennas Wireless Propag. Lett.*, vol. 10, pp. 666–669, 2011.

[11] R. K. Chaudhary, K. V. Srivastava, and A. Biswas, "A practical approach: Design of wideband cylindrical dielectric resonator antenna with permittivity variation in axial direction and its fabrication using microwave laminates," *Microw. Opt. Technol. Lett.*, vol. 55, no. 10, pp. 2282–2288, Oct. 2013.

[12] R. Chowdhury, R. Kumar, and R. K. Chaudhary, "A new technique to enhance the impedance bandwidth of CDRA using drilling holes," in *Proc. 11th Int. Conf. Ind. Inf. Syst. (ICIIS)*, Dec. 2016, pp. 259–262.

[13] Y. Lin Zhang, W. Hong, F. Xu, K. Wu, and T. Jun Cui, "Analysis of guided-wave problems in substrate integrated waveguides -numerical simulations and experimental results," in *IEEE MTT-S Int. Microw. Symp. Dig.*, Philadelphia, PA, USA, Jul. 2003.

[14] F. Xu and K. Wu, "Numerical multimode calibration technique for extraction of complex propagation constants of substrate integrated waveguide," in *IEEE MTT-S Int. Microw. Symp. Dig.*, vol. 2, Fort Worth, TX, USA, Jun. 2004, pp. 1229–1232.

[15] L. Sun, B. Sun, J. Yuan, W. Tang, and H. Wu, "Low-profile, quasi-omnidirectional substrate integrated waveguide (SIW) multihorn antenna," *IEEE Antennas Wireless Propag. Lett.*, vol. 15, pp. 818–821, 2016.
[16] Q. Wu, J. Yin, C. Yu, H. Wang, and W. Hong, "Broadband planar SIW cavity-backed slot antennas aided by unbalanced shorting vias," *IEEE Antennas Wireless Propag. Lett.*, vol. 18, no. 2, pp. 363–367, Feb. 2019.
[17] M. S. H. S. El-Din, H. El-Hennawy, A. M. M. A. Allam, S. I. Shams, M. S. H. S. El-Din, M. F. A. Sree, and A. Gaafar, "Approach for determination of the stop band for ridge gap waveguide," in *Proc. 7th Int. Conf. Electr. Electron. Eng. (ICEEE)*, Antalya, Turkey, Apr. 2020, pp. 72–75.
[18] S. I. Shams and A. A. Kishk, "Determining the stopband of a periodic bed of nails from the dispersion relation measurements prediction," *IEEE Trans. Compon., Packag., Manuf. Technol.*, vol. 7, no. 4, pp. 621–629, Apr. 2017.
[19] M. M. M. Ali and A.-R. Sebak, "2-D scanning magnetoelectric dipole antenna array fed by RGW Butler matrix," *IEEE Trans. Antennas Propag.*, vol. 66, no. 11, pp. 6313–6321, Nov. 2018, doi: 10.1109/TAP.2018.2869228.
[20] A. Dadgarpour, M. S. Sorkherizi, and A. A. Kishk, "Wideband low-loss magnetoelectric dipole antenna for 5G wireless network with gain enhancement using meta lens and gap waveguide technology feeding," *IEEE Trans. Antennas Propag.*, vol. 64, no. 12, pp. 5094–5101, Dec. 2016.
[21] D. Shen, C. Ma, W. Ren, X. Zhang, Z. Ma, and R. Qian, "A low-profile substrate-integrated-gap-waveguide- fed magnetoelectric dipole," *IEEE Antennas Wireless Propag. Lett.*, vol. 17, no. 8, pp. 1373–1376, Aug. 2018.
[22] A. Dadgarpour, N. Bayat-Makou, M. A. Antoniades, A. A. Kishk, and A. Sebak, "A dual-polarized magnetoelectric dipole array based on printed ridge gap waveguide with dual-polarized split-ring resonator lens," *IEEE Trans. Antennas Propag.*, vol. 68, no. 5, pp. 3578–3585, May 2020.
[23] N. Ashraf, A. R. Sebak, and A. A. Kishk, "Packaged microstrip line feed network on a single surface for dual-polarized 2N×2M ME-dipole antenna array," *IEEE Antennas Wireless Propag. Lett.*, vol. 19, no. 4, pp. 596–600, Apr. 2020.
[24] M. B. Kakhki, A. Dadgarpour, M. A. Antoniades, A.-R. Sebak, and T. A. Denidni, "Dual complementary source magneto-electric dipole antenna loaded with split ring resonators," *IEEE Access*, vol. 8, pp. 59351–59361, 2020.
[25] H. Attia and A. A. Kishk, "Wideband self-sustained DRA fed by printed ridge gap waveguide at 60 GHz," in *Proc. IEEE 28th Annu. Int. Symp. Pers., Indoor, Mobile Radio Commun. (PIMRC)*, Montreal, QC, Canada, Oct. 2017, pp. 1–3.
[26] M. B. Kakhki, A. Dadgarpour, A. Sebak, and T. A. Denidni, "Twenty-eight-gigahertz beam-switching ridge gap dielectric resonator antenna based on FSS for 5G applications," *IET Microw., Antennas Propag.*, vol. 14, no. 5, pp. 397–401, Apr. 2020.
[27] H. A. Malhat and S. H. Zainud-Deen, "Circularly polarized ridge gap waveguide fed SIW dielectric resonator antenna," in *Proc. 7th Int. Japan–Africa Conf. Electron., Commun., Comput. (JAC-ECC)*, Alexandria, Egypt, Dec. 2019, pp. 144–147.
[28] J. F. J. Veldhuijzen van Zanten, G. A. Schuerink, A. H. J. Tullemans, R. Legtenberg, and W. W. Wits, "Method to determine thermoelastic material properties of constituent and copper-patterned layers of multilayer printed circuit boards," *J. Mater. Sci., Mater. Electron.*, vol. 29, no. 6, pp. 4900–4914, Mar. 2018.

MOHAMED MAMDOUH M. ALI (Member, IEEE) received the B.Sc. (Hons.) and the M.Sc. degrees in electronics and communications engineering from Assiut University, Egypt, in 2010 and 2013, respectively, and the Ph.D. degree in electrical and computer engineering from Concordia University, Montreal, QC, Canada, in 2020. From 2010 to 2015, he was a Teaching and Research Assistant with the Department of Electronics and Communications Engineering, Assiut University. From 2015 to 2020, he was a Teaching and Research Assistant with the Department of Electrical and Computer Engineering (ECE), Concordia University. From 2020 to 2021, he was a Research Associate with the Institut National de la Recherche Scientifique (INRS), University of Quebec, Montreal. He is currently a Research Associate with the PolyGrames Research Center, Department of Electrical Engineering, Ecole Polytechnique de Montréal, Montreal University, Canada. His research interests include millimeter-wave antennas for 5G/6G applications, analog and hybrid beamforming networks, dielectric resonator antennas, microstrip antennas, multi-function antennas, microwave circuits, electromagnetic bandgap (EBG), artificial magnetic conductors, soft and hard surfaces, frequency selective surfaces, reflect/transmitarray, and non-reciprocal microwave devices. He received the Distinction with Honor from Assiut University, in 2010. He was a recipient of Egyption Government Mission Scholarship, in 2015. He was a recipient of the Concordia University Recruitment Award, in 2016, and the Concordia University Accelerator Award, in 2019. He received the NSERC CREATE Training Program in Pervasive and Smart Wireless Applications for the Digital Economy (PERSWADE), in 2018. Recently, he received a recipient of Nature et technologies (FRQNT) Postdoctoral research scholarship, in 2021.

MUATH AL-HASAN (Senior Member, IEEE) received the B.A.Sc. degree in electrical engineering from the Jordan University of Science and Technology, Jordan, in 2005, the M.A.Sc. degree in wireless communications from Yarmouk University, Jordan, in 2008, and the Ph.D. degree in telecommunication engineering from the Institut National de la Recherche Scientifique (INRS), Université du Québec, Canada, 2015. From 2013 to 2014, he was with Planets Inc., California, USA. In May 2015, he joined Concordia University, Canada, as Postdoctoral Fellowship. He is currently an Assistant Professor with Al Ain University, United Arab Emirates. His current research interests include antenna design at millimeter-wave and Terahertz bands, channel measurements in multiple-input and multiple-output (MIMO) systems, CAD and modeling of microwave and antenna structures, and numerical analysis.

ISMAIL BEN MABROUK (Senior Member, IEEE) received the B.A.Sc. and M.A.Sc. degrees in electrical engineering from the University of Lille, Lille, France, in 2006 and 2007, respectively, and the Ph.D. degree in electrical engineering from the University of Quebec, Canada, in 2012. From 2007 to 2009, he was with Huawei Technologies, Paris, France. In 2012, he joined the Wireless Devices and Systems (WiDeS) Group, University of Southern California, Los Angeles, USA. He is currently an Assistant Professor with Durham University, Durham, U.K. His research interests include antenna design at the millimeter-wave and THz frequencies, propagation studies for multiple-input and multiple-output (MIMO) systems, deep learning, and wireless body area network for medical applications. He is a recipient of the Abu Dhabi Award for Research Excellence (AARE).

TAYEB A. DENIDNI (Fellow, IEEE) received the M.Sc. and Ph.D. degrees in electrical engineering from Laval University, Quebec City, QC, Canada, in 1990 and 1994, respectively. From 1994 to 2000, he was a Professor with the Engineering Department, Université du Québec á Rimouski (UQAR), Rimouski, QC, Canada, where he founded the Telecommunications laboratory. Since 2000, he has been with the Institut National de la Recherche Scientifique (INRS), University of Quebec, Montreal, QC, Canada. He founded the RF Laboratory, INRS—Energie, Materiaux et Telecommunications (INRS-EMT), Montreal. He has extensive experience in antenna design. He served as a principal investigator for many research projects sponsored by NSERC, FCI, and numerous industries. His current research interests include reconfigurable antennas using electromagnetic bandgap and frequency-selective surface structures, dielectric resonator antennas, meta- material antennas, adaptive arrays, switched multi-beam antenna arrays, ultrawideband antennas, microwave, and development for wireless communications systems.